Estimating the Reliability of the Inspection System Employed for Detecting Defects in Rail Track Using Ultrasonic Guided Waves

Abdelgalil Khalil, Faeez Masurkar, and A. Abdul-Ameer(✉)

Faculty of Engineering and IT, The British University in Dubai, Block 11, 1st and 2nd Floors, Dubai International Academic City, Dubai, United Arab Emirates
alaa.ameer@buid.ac.ae

Abstract. This work focuses on the implementation of a data-based method to determine the inspection system reliability in terms of detecting different types of damages in rail tracks using ultrasonic-guided Rayleigh waves and a probability of detection (POD) technique. In this study, the reliability is tested against a surface crack (SC) and sub-surface damage – a through-side thickness hole (TSTH). The guided Rayleigh waves are generated using a custom-designed sensor that excites Rayleigh surface waves in the specimen and the propagating waves are sensed on the rail track surface. The wedge shape design of the sensor helps to excite a specific ultrasonic mode in the sample thereby hindering the ultrasonic energy of other coupled guided waves that can propagate simultaneously and the wedge angle is determined according to Snell's law relying on the wave velocity of Rayleigh wave and bulk longitudinal wave. The guided wave responses as a function of varying severity of defects are obtained through a simulation study after the verification of the obtained guided wave responses with the help of an experimental study. A damage index (DI) is defined depending on defect size that gives the trend of damage severity from the captured ultrasonic responses and for monitoring defects in the rail track. This DI is eventually fed into the POD model to determine the probability of defect detection which in turn helps determine the inspection system reliability. The POD method also helps to study the critical design parameters that could affect or improve crack detection results.
Purpose – To determine the reliability of inspection system deployed for interrogating health status of rail track.
Methodology – Employing the Probability of detection technique for determining how reliable the inspection system is in detecting the health status of the rail track specimen using the ultrasonic guided waves.
Findings – It has been found that the proposed inspection system is >90% reliable in detecting defects.
Implications – This methodology can help maintenance engineers to make an informed decision on their developed technique for investigating the health status of the rail track sample.
Originality/ value – 13%.

Keywords: Rayleigh-waves · probability of detection · damage estimation · wedge sensors · Rail track specimens

K. Al Marri et al. (Eds.): *BUiD Doctoral Research Conference 2023*, LNCE 473, pp. 190–202, 2024.
https://doi.org/10.1007/978-3-031-56121-4_19

Nomenclature

$C_R, C_L, C_T =$ Rayleigh, Longitudinal, Transverse velocity.
$\lambda, \mu =$ Lame's constants; $\nu =$ Poisson's ratio
$\rho =$ Material density; $E =$ Elastic Modulus
$I_R =$ Incident Rayleigh wave; $I_d^R =$ Damage reflected Rayleigh wave; $\lambda_R =$ Wavelength of Rayleigh wave

1 Introduction

Non-Destructive testing (NDT) systems are gaining worldwide attention by several researchers as they can detect surface and sub-surface defects without destroying the inspected component and offering good accuracy. The inspection is conducted using sensors permanently attached at the known critical locations of the specimen. The recorded data is processed using different algorithms to extract useful information.

There is an increasing attention worldwide for High-speed railways as being a timely means of transportation. However, the rail tracks are subjected to constant and fluctuating loads over different times of service which results in development of micro and macro scale damages in the rail material especially on surface. This will consequently decrease its load bearing ability and eventually result in failure and de-railing resulting into loss of economy and human life (Kim & Hoon & Woo 2012, Masurkar & Yelve 2017).

There are several NDT techniques available to inspect rail damage such as visual, contact, and non-contact ultrasound, eddy current, magnetic particles test, x-ray, and non-contact laser ultrasound-based scanning techniques. A large portion of the inspection is conducted with labour intensive visual inspection which is time consuming. For long range inspections, vehicles integrated with laser scanning devices or visual cameras have been utilized and commercialized. However, vision-based devices can only detect surface damages and accuracy highly dependent on the image quality and also affected by the outside weather conditions whereas laser-based ultrasound scanning can detect surface and embedded damages – shelling, sub-surface damages, etc. (Heckel & Wack & Mook 2019, Masurkar & Yelve 2022).

Of the several approaches, ultrasound-based NDT has gained widespread recognition as they can be excited and sensed by cost effective sensors and easily affixed to the specimen. Furthermore, non-contact sensors are available to improve the speed of data acquisition and repeatability of the measurements. Despite these advantages, ultrasound-based NDT suffers from a couple of drawbacks as following. First, the ultrasonic waves are highly dispersive and a thorough study of different guided and coupled wave modes must be conducted through dispersion analysis to design the simulation and experimental study. The method of actuation and sensing should be carefully adopted for high quality data acquisition. Nonetheless, the wave propagation physics could be simplified if actuation and sensing strategy is carefully developed (Masurkar et al. 2021, Masurkar & Rostami & Tse 2020).

(Janapati et al. 2016) discussed the estimation of POD for a metallic specimen using ultrasonic guided waves. (Forsyth 2016) discussed the POD principle using several inspections and experimental data. (Meeker & Roach & Kessler 2019) discussed how

effectively the POD can be applied to NDT studies. (Virkkunen et al. 2019) presented a comparison between hit/miss and â versus a for different ultrasonic wave-based data sets. (Cobb & Fisher & Michaels 2009) presented a case study concerning the implementation of POD curves using a model-based formulation. (Mishra & Yadav & Chang 2019) studied the POD method using the acousto-ultrasound quantified as "in-situ NDE" for detection of fatigue crack.

This work focusses on reliability estimation of inspection system employed for the NDT of a rail track using ultrasonic waves. The crack presence and progression are determined quantitatively using the POD method that helps to estimate the system reliability. Based on the dispersion curves, an excitation frequency is selected to conduct the simulation and experimental study. From the time-domain signals acquired for incremental progressions of crack, a DI curve is constructed to quantify the progression of SC and TSTH in the specimen. As a last step to determine the reliability, POD curve is constructed from the DI curve based on the mean and variance estimates that also predicts probability associated with each damage.

The organization of paper is as follows. First, the Introduction and background are given in Sect. 1, then the methodology and material description in Sects. 2 and 3 respectively. The details on the numerical and experimental studies in Sects. 4 and 5 respectively. The results are discussed in Sect. 6. Finally, the concluding remarks in Sect. 7.

2 Methodology

In this study, emphasis is on reliability estimation of the inspection system employed to detect SC & TSTH damages in rail track. Firstly, strategy is developed to generate and receive only the Rayleigh mode propagating within the specimen. The detection is conducted using wedge sensor and the pulse-echo configuration. The data is recorded for pristine specimen and later at different incremental progressions of damage. Further, a DI is determined from the recorded responses, and fed in the POD model to predict the system reliability and probability of each damage size that can be detected.

2.1 Theoretical Model of Probability of Detection Technique

Suppose 'a' being the true size of crack, '$\hat{a}$' be the calibrated size, and 'x' and 'y' is the natural log of the true and calibrated sizes respectively. The linear relationship is written as (Annis et al. 2009),

$$y = \beta_0 + \beta_1 x + \epsilon; \tag{1}$$

here 'ϵ' is the residual between the fitting and true data and has a gaussian distribution with mean $\mu = 0$ and 'δ^2' as its variance. The standard normal variate is,

$$Z = \frac{y - (\beta_0 + \beta_1 x)}{\delta}; \tag{2}$$

which has a normal distribution as,

$$\phi(z) = \frac{1}{\sqrt{2\pi}} e^{\frac{-Z}{2}^2} \tag{3}$$

The normal distribution has a cumulative distribution function (CDF) that is,

$$Q(z) = \int_{z}^{\infty} \phi(Z)dz \tag{4}$$

Thus, the POD associated to a specific crack size is,

$$\text{POD}(x) = \text{POD}(y > y_{th}) = Q\left[\frac{y_{th} - (\beta_0 + \beta_1 x)}{\delta}\right] \tag{5}$$

where, y_{th} is the detection threshold. The CDF complement is,

$$Q[-Z] = 1 - Q[Z] \tag{6}$$

$$\begin{aligned}\text{POD}\,(a) = \text{POD}\,(y > y_{th}) &= 1 - Q\left[\frac{x - \left(\frac{y_{th}-\beta_0}{\beta_1}\right)}{\frac{\delta}{\beta_1}}\right] \\ &= 1 - Q\left[\frac{\log_e(a) - \left(\frac{y_{th}-\beta_0}{\beta_1}\right)}{\frac{\delta}{\beta_1}}\right]\end{aligned} \tag{7}$$

Thus, mean $= \left(\frac{y_{th}-\beta_0}{\beta_1}\right)$ and standard deviation $= \frac{\delta}{\beta_1}$ which is used for estimating the POD curve versus true crack size.

3 Theory and Material Description

In this work, ultrasonic Rayleigh waves are employed for NDT of rail track. The fundamental background of Rayleigh waves is presented in the following sub-section.

3.1 Rayleigh Waves

Rayleigh surface waves are elastic waves having both longitudinal and transverse displacements and propagate only near the surface. Therefore, their energy decreases as the sensing point moves away from the surface. The governing equation of a Rayleigh wave is given as,

$$\eta^6 - 8\eta^4 + 8\eta^2\left(3 - 2\zeta^2\right) + 16\left(\zeta^2 - 1\right) = 0, \tag{8}$$

where,

$$\zeta = \frac{C_T}{C_L} = \sqrt{\frac{1 - 2\nu}{2(1 - \nu)}} \tag{9}$$

and $\eta = \frac{C_R}{C_T}$. The alternate solution of η is $(0.87 + 1.12\nu)/(1 + \nu)$. Thus, the Rayleigh wave velocity can be calculated as,

$$C_R = \left(\frac{0.87 + 1.12\nu}{1 + \nu}\right)C_T, \tag{10}$$

From Eq. 10, the Rayleigh velocity is free of excitation frequency f, and thus they are non-dispersive.

3.2 Material Properties of Specimen

The specimen used is a section of real rail track of the high-speed train as shown in Fig. 2. Normally rail track specimens are full of rust and to get the baseline measurements, the specimen was polished before employing it for the experimental study. Initially a hand grinder was used to remove the rust and later a fine sandpaper used to improve the surface quality. In particular, the surface portion of the rail track is always rust-free as it is in contact with the wheels of the train. This helps to acquire the wave propagation data with a higher signal-to-noise ratio (SNR). The material properties of the specimen are given in Table 1.

Table 1. Material properties of the Rail track

Mechanical properties	Value
ρ (kg/m^3)	7799
E (GPa)	212
$\nu(-)$	0.2866
λ (GPa)	110.7
μ (GPa)	82.4

The Lame's constants are obtainable from elastic modulus and Poisson's ratio as, $\lambda = \frac{E\nu}{(1-2\nu)(1+\nu)}$ and $\mu = \frac{E}{2(1+\nu)}$. Further, the bulk wave velocities can be determined using the Lame's constants and density as, $C_L = \sqrt{\frac{\lambda+2\mu}{\rho}}$ and $C_T = \sqrt{\frac{\mu}{\rho}}$. The Lame's constants and the wave velocities are shown in Table.1 and 2 respectively.

Table 2. Wave velocities in the Rail track

Type of wave	Value (m/s)
Rayleigh	3008.911
Longitudinal	5943.487
Shear	3250.455

3.3 Dispersion Analysis of the Rail Track

The possible propagation of several modes in the rail track as a function of different excitation frequencies can be determined using the dispersion curves in Fig. 1. Therefore, dispersion curves are first obtained for the rail specimen considering the upper portion of the specimen as a thick rectangular steel bar since the propagation of guided wave is limited to only the upper portion of the rail track. Due to higher thickness (~50 mm) of

the specimen surface, guided Rayleigh wave propagated in the specimen, and it has good penetration depth to detect any sub-surface flaws in the specimen. This is also confirmed by the wave structure analysis.

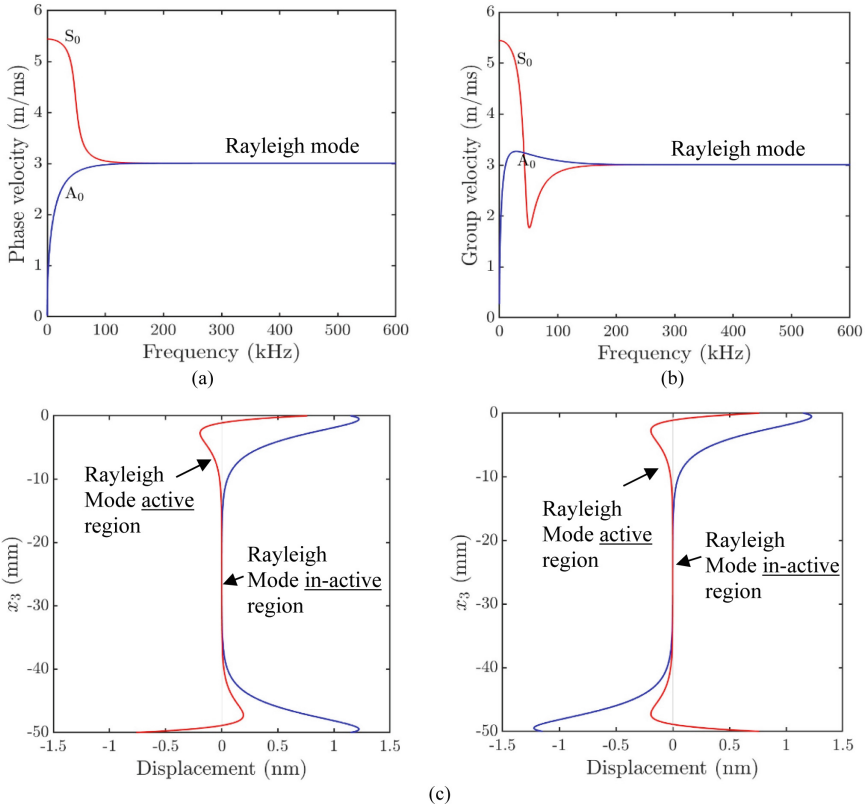

Fig. 1. Dispersion curves of rail track (a) Phase (b) Group (c) analysis of Rayleigh wave displacement.

4 Finite Element (FE) Study

4.1 The FE Model Setup

In order to excite Rayleigh waves in the specimen, a plexiglass wedge is modeled in the simulation as shown in Fig. 2. The angle required to excite the Rayleigh wave in the specimen is calculated as the inverse sin of the longitudinal velocity in the wedge over the Rayleigh velocity in the specimen. The wedge is modeled at a distance of 190 mm from the nearest end to correlate results with the experiments.

The excitation applied at the flank of wedge is a 6.5 cycles sine wave modulated with gaussian function and a central frequency of 500 kHz. This applied excitation signal in

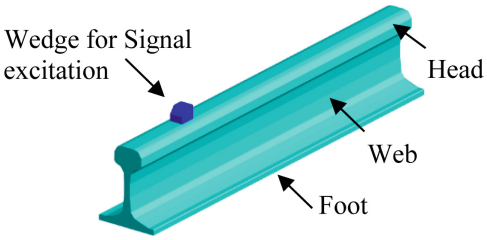

Fig. 2. Schematic diagram of FE model.

time and frequency domain can be seen in Fig. 3. For this frequency, a penetration depth of 6 mm can be achieved which is also equal to the wavelength of the Rayleigh wave. Thus, a Rayleigh wave signal launched into the rail track specimen at this frequency could be useful to interrogate the surface or subsurface damages.

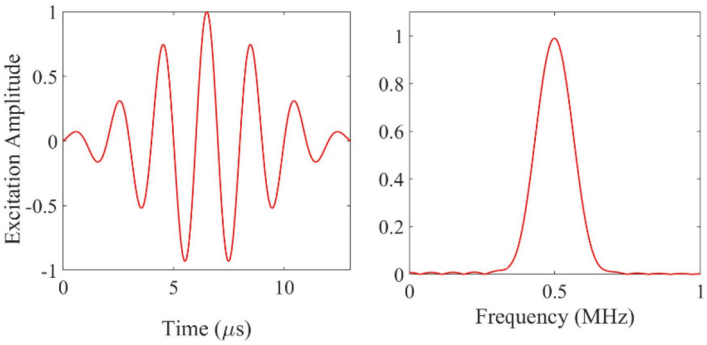

Fig. 3. Excitation signal in time and frequency domain.

5 Experimental Study

The experimental setup is fully non-contact comprising an actuation laser and a three dimensional (3D) receiving laser. Since a raw laser beam will induce multiple wave modes simultaneously into the specimen, a slit mask coupled with optics setup arrangement is used to convert the beam into a series of multiple laser lines (Masurkar & Rostami & Tse 2020). This ensures a generation of pure Rayleigh wave into the specimen and the frequency is determined by the spacing between each laser line as shown in Fig. 4. At the receiving end, a 3D scanning laser doppler vibrometer (SLDV) is used to capture the Rayleigh wave propagation exhibiting x, y, and z displacements. The schematic of the complete experimental setup and the equipment's used is shown in Fig. 4.

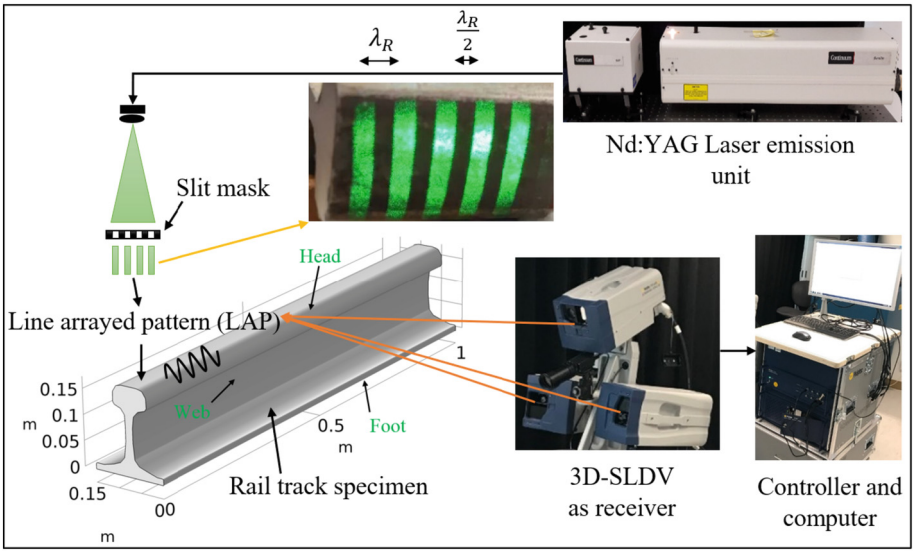

Fig. 4. Experimental setup for verification (Masurkar & Rostami & Tse 2020)

6 Results and Discussions

In this section, the results obtained from the study are discussed. Firstly, the results from an intact specimen are presented. The wave animation over two different time instants for a pristine rail track sample can be seen in Fig. 5. The longitudinal wave excited at the wedge flank at a crtical angle of 47.4^0, generates a pure Rayleigh wave in the specimen which then propagates along the surface.

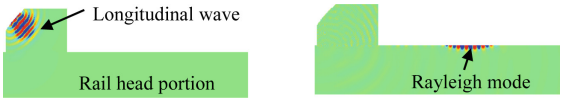

Fig. 5. Wave propagation showing generation of bulk wave in wedge and Rayleigh wave in Rail track specimen [side view]

Next, the results from experiments at intact state are presented for measurements conducted at different times. As a result of the surface conditions of the specimen as well as the repeatability issues associated with the use of the excitation Laser, the signals received using the laser system at different times are compared to check the variation between each of them. Thus, the repeatability of the experimental results is firstly verified and is presented in Fig. 6. Certainly, there are variations in the measurements – M1, M2, & M3. Thus, an effective signal processing method (Masurkar & Rostami & Tse 2020) namely Self adaptive smart algorithm (SASA) was applied to each of the recorded responses. SASA is based on the concept that a reflection of the incident wave caused by any irregularity (defect) or boundary in the specimen will exhibit almost similar shape

of the incident wave and thereby yield a maximum correlation. SASA is effective in suppressing high levels of noise while keeping only useful time-domain signal. One of the signals processed with SASA is shown in Fig. 6. The filtered signal is now fully free of noise and is dominated by the incident wave packet. There are no potential reflections as it's an intact specimen, and the excitation and sensing are optimized to minimize the reflections from the specimen boundaries.

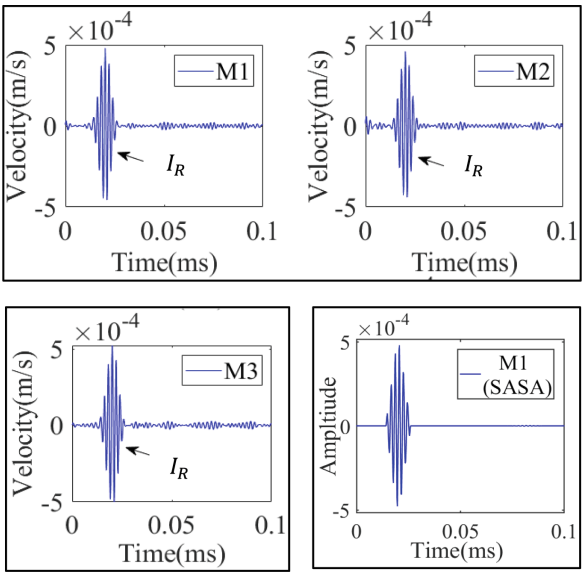

Fig. 6. Time domain responses for intact sample and SASA filtering.

Figure 7 shows the schematic of the actuation and sensing on the rail track specimen for both types of damages – SC and TSTH. Figure 8 shows the experimentally obtained time domain signal in presence of SC. Now the fidelity of built simulation model is verified with reference to these experimental results so that all results obtained through simulations could be confirmed to be obtainable in practice.

Figure 9 shows the simulation obtained time domain signal that shows good correlation with the experimentally obtained time domain signals as seen in Fig. 8.

After this verification, the FE simulations are conducted for increasing SC and TSTH in the specimen and responses are captured in the pulse echo mode for in and out-plane motion. For brevity, the ultrasonic responses for different damage sizes are not shown here. Instead, only the major results are presented. For a damaged specimen, wave is reflected from the damage and is sensed in the pulse echo mode. Thus, an index is defined that quantifies the discrepancies between the pristine and damaged state responses. The damage index (DI) used here is shown in Eq. 8 as follows,

$$DI = \frac{\sum_{n=1}^{N}[E_{Current}(n) - E_{Baseline}(n)]^2}{\sum_{n=1}^{N}[E_{Baseline}(n)]^2} \tag{11}$$

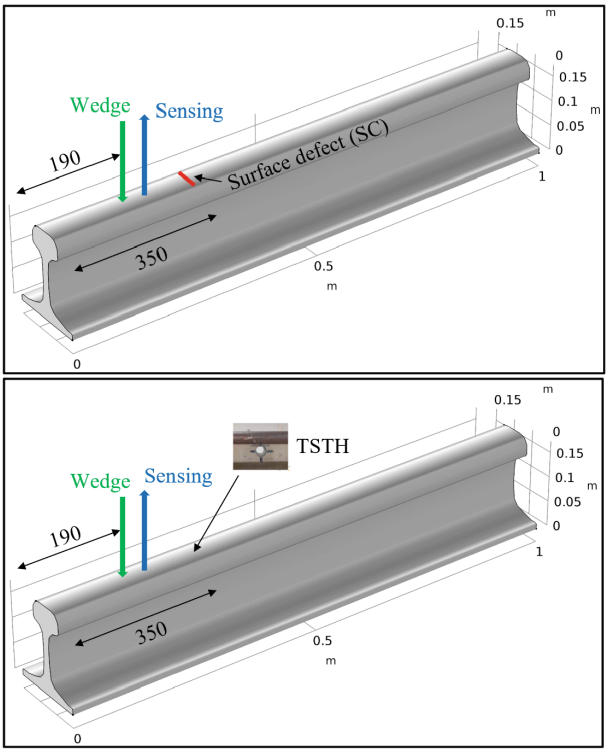

Fig. 7. Schematic of excitation, sensing & defect location

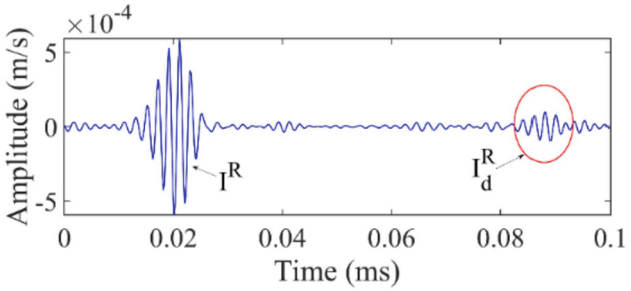

Fig. 8. Time domain waveform from experimental studies - Ext-End: 190 mm; Ext-Sensing: 60 mm; Ext-Defect: 160

where $E_{Current}$ is the response at the current state and $E_{Baseline}$ is the pristine condition response, and n being the samples in response. The DI is then calculated using the in and out plane responses captured at pristine and damaged states for incremental severity using Eq. 8. And is shown in Fig. 10. The DI curve is seen to increase with increase in sizes of SC. Further, a linear regression is employed that gives the mean and standard deviation parameters in Eq. 7, as well as variance and other parameters of the POD

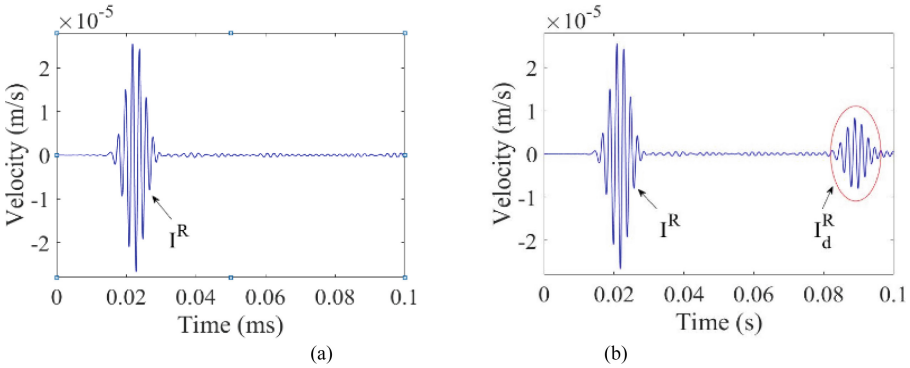

Fig. 9. Time domain waveforms from simulation studies (a) Intact (b) Ext-End: 190 mm; Ext-Sensing: 60 mm; Ext-Defect: 160

model. Thus, the POD curve is developed for the in and out plane responses for both type of damages – SC and TSTH. For brevity, the POD curves for only in-plane motion are shown in Fig. 11 for both damages.

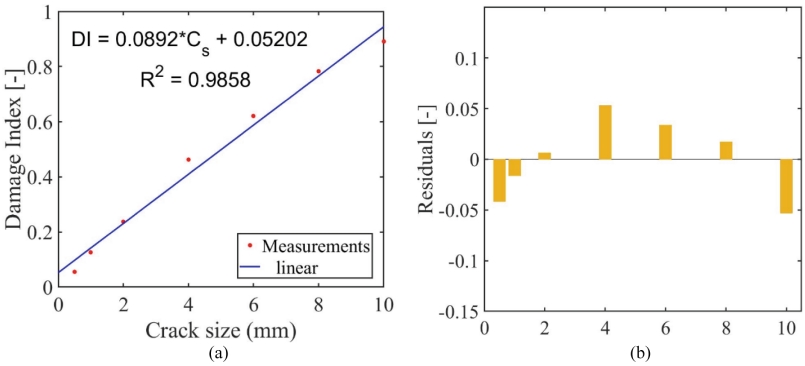

Fig. 10. (a) Damage Index versus Crack size - SC (b) Residuals for different crack size - SC

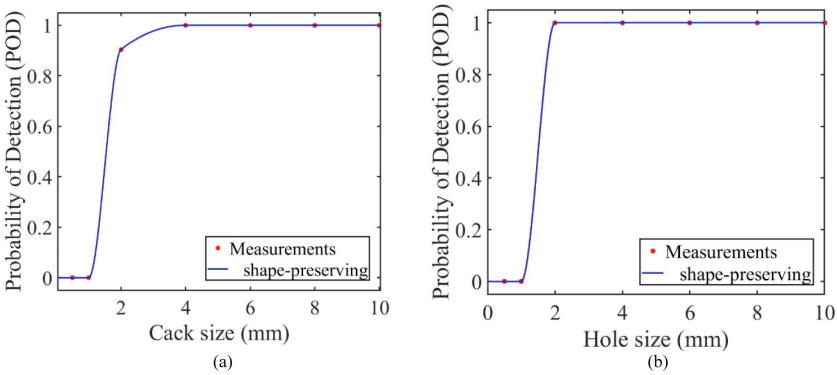

Fig. 11. POD estimation (a) SC (b) TSTH

7 Summary

This work focussed on determining the reliability of the system employed for inspecting structural integrity of rail track specimen using Rayleigh waves which were actuated using a wedge sensor and sensed at a specific location on the specimen surface for different progressions of SC and TSTH. The received time domain signals were used to estimate the DI curves as a function of damage sizes, and this was processed using the POD algorithm to determine system reliability further yielding the probability associated with each damage size. The results show that proposed inspection system and the strategy found after conducting multiple simulations duly supported with experimental study can be helpful for inspecting rail track specimens in a reliable manner.

The concluding remarks can be summarized as below:

1. The employed guided Rayleigh wave can detect the incremental SC & TSTH damages in the rail track sample.
2. The DI curve determined based on the guided wave data is very helpful to quantify the progressions of damages.
3. The POD curves yield the reliability of the employed inspection system and can reveal specific system parameters that could further help in improving system reliability.

References

Kim, N.H., Hoon, S., Woo, H.S.: Rail inspection using noncontact laser ultrasonics. J. Korean Soc. Non-destruct. Test. **32**(6), 696–702 (2012)

Masurkar, F.M., Yelve, N.P.: Optimizing location of damage within an enclosed area defined by an algorithm based on the Lamb wave response data. Appl. Acoust. **120**, 98–110 (2017)

Heckel, T., Wack, Y., Mook, G.: Simulation of an instrumented ultrasonic test run with a rail inspection train. Rev. Progr. Quant. Non-destruct. Eval. (2019)

Masurkar, F.M., Yelve, N.P., Tse, P.: Nondestructive testing of rails using nonlinear Rayleigh waves. Proc. Inst. Mech. Eng. C J. Mech. Eng. Sci. **236**(15), 8527–8541 (2022)

Masurkar, F.M., Ng, K.M., Tse, P., Yelve, N.P.: Interrogating the health condition of rails using the narrowband Rayleigh waves emitted by an innovative design of non-contact laser transduction system. Struct. Health Monit. **20**(5), 2678–2693 (2021)

Masurkar, F.M., Rostami, J., Tse, P.: Design of an innovative and self-adaptive-smart algorithm to investigate the structural integrity of a rail track using Rayleigh waves emitted and sensed by a fully non-contact laser transduction system. Appl. Acoust. **166** (2020)

Janapati, V., Kopsaftopoulos, F., Li, F., Lee, S.J., Chang, F.K.: Damage detection sensitivity characterization of acousto-ultrasound-based structural health monitoring techniques. Struct. Health Monit. **15**, 143–161 (2016)

Forsyth, D.S.: Structural health monitoring and probability of detection estimation. In: AIP Conference Proceedings, vol. 1706 (2016)

Meeker, W.Q., Roach, D., Kessler, S.S.: Statistical methods for probability of detection in structural health monitoring. In: International Workshop on Structural Health Monitoring (2019)

Virkkunen, I., Koskinen, T., Papula, S., Sarikka, T., Hänninen, H.: Comparison of â versus a and hit/miss POD estimation methods: a European viewpoint. J. Nondestruct. Eval. **38** (2019)

Cobb, A.C., Fisher, J., Michaels, J.E.: Model-assisted probability of detection for ultrasonic structural health monitoring. In: Proceedings of the 4th European-American workshop on Reliability of NDE, Berlin, Germany, pp. 24–26 (2009)

Mishra, S., Yadav, S.K., Chang, F.K.: Reliability of probability of detection of fatigue cracks for built-in acousto-ultrasound technique as in-situ NDE. Struct. Health Monit. (2019)

Annis, C., Bray, E., Hardy, H., Hoppe, P.M.: Nondestructive evaluation system reliability assessment. United States Department of Defense. Handbook MIL-HDBK-1823A (2009)